

# VLBA monitoring of Mrk 421 at 15 and 24 GHz during 2011

R. Lico, M. Orienti, G. Giovannini

*Dipartimento di Astronomia, Università di Bologna, 40127 Bologna, Italy*

M. Giroletti

*INAF Istituto di Radioastronomia, 40129 Bologna, Italy*

B. Cotton

*National Radio Astronomy Observatory, Charlottesville, VA 22903-2475, USA*

P. G. Edwards

*CSIRO Australia Telescope National Facility, Marsfield, NSW 2122, Australia*

L. Fuhrmann, T. P. Krichbaum

*Max-Planck-Institut für Radioastronomie, Auf dem Hügel 69, 53121 Bonn, Germany*

K. Sokolovsky, Y. Kovalev

*Astro Space Center of the Lebedev Physical Institute, 117997 Moscow, Russia*

S. Jorstad, A. Marscher

*Institute for Astrophysical Research, Boston University, Boston, MA 02215, USA*

M. Kino

*National Astronomical Observatory of Japan, Osawa 2-21-1, Mitaka, Tokyo 181-8588*

D. Paneque

*Max-Planck-Institut für Physik, D-80805 München, Germany*

M. A. Perez-Torres

*Instituto de Astrofísica de Andalucía, IAA-CSIC, 18080 Granada, Spain*

G. Piner

*Department of Physics and Astronomy, Whittier College, Whittier, CA, USA*

We present a preliminary analysis of new high resolution radio observations of the nearby TeV blazar Markarian 421 ( $z=0.031$ ). This study is part of an ambitious multifrequency campaign, with observations in sub-mm (SMA), optical/IR (GASP), UV/X-ray (Swift, RXTE, MAXI), and  $\gamma$  rays (Fermi-LAT, MAGIC, VERITAS). In this manuscript we consider only data obtained with the Very Long Baseline Array (VLBA) at seven epochs (one observation per month from January to July 2011) at 15 and 23.8 GHz. We investigate the inner jet structure on parsec scales through the study of model-fit components for each epoch. We identified 5-6 components which are consistent with being stationary during the 6-month period reported here. The aim is to try to shed light on questions such as the nature of radiating particles, the connection between radio and  $\gamma$ -ray emission, the location of emitting regions and the origin of the flux variability.

## 1. Introduction

Markarian 421 (R.A.= $11^h04^m27.31^s$ , decl.= $+38^\circ 12' 31.8''$ ) is one of the nearest ( $z=0.031$ ) and one of the brightest BL Lac objects in the sky. It was the first extragalactic source detected at TeV energies by the Cherenkov telescope at Whipple Observatory [1]. The spectral energy distribution (SED) of this object, dominated by non-thermal emission, shows two smooth broad components: one at lower energies, from radio band to soft X-ray domain, and one at higher energies peaking at  $\gamma$ -ray energies [2]. The low-frequency peak is certainly due to synchrotron emission from relativistic electrons in the jet interacting with magnetic field; the high-frequency peak is probably due to inverse Compton scattering of the same population of relativistic electrons with synchrotron low energy photons (Synchrotron Self Compton model)[2, 3]. So we might expect to find an X-ray/ $\gamma$ -ray correlation. Mrk 421 shows variability at all frequencies; particularly at TeV energies Gaidos et al. [4] measured a variability of  $\sim 15$  minutes.

At radio frequencies this source clearly shows a one-

sided jet structure aligned at a small angle with respect to the line of sight [5]. In this work we present new VLBA (Very Long Baseline Array) observations to study in detail the inner jet structure on parsec scales. We can investigate the evolution of shocks that arise in the jet, with model-fitting techniques. In many works [6, 7] jet components show only subluminal apparent motion, and this seems to be a common characteristic of TeV Blazars. Thanks to accurate measurements of changes on parsec scales, by the VLBA, we can find valid constraints on the geometry and kinematics of the jet. Despite several accurate studies on this source [2], details of physical processes responsible for the observed emission are still poorly constrained. Because of its strong variability and broadband spectrum, multiwavelength long term observations are required for a good comprehension of emission mechanisms.

This study is part of an ambitious multi-year and multi-instrument campaign, which also involves observations in sub-mm (SMA), optical/IR (GASP), UV/X-ray (Swift, RXTE, MAXI), and  $\gamma$  rays (Fermi-LAT, MAGIC, VERITAS). The aim of this observational effort is to try to shed light on fundamental

Observation date	Map Peak (mJy/beam)		Beam (mas x mas)		Lowest contour (mJy/beam)		Notes
	15GHz	23.8GHz	15GHz	23.8GHz	15GHz	23.8GHz	
2011/01/14	340	316	0.89 x 0.52	0.73 x 0.41	1.0	1.0	No MK, no NL
2011/02/25	391	335	1.09 x 0.70	0.58 x 0.35	0.8	0.7	NL snowing
2011/03/29	384	358	0.93 x 0.55	0.61 x 0.36	1.2	1.1	No HK
2011/04/25	358	305	0.89 x 0.50	0.56 x 0.32	1.1	0.9	-
2011/05/31	355	295	0.90 x 0.52	0.58 x 0.34	1.1	0.9	-
2011/06/29	260	207	0.85 x 0.49	0.56 x 0.32	1.0	0.8	No LA
2011/07/28	228	192	0.87 x 0.51	0.52 x 0.34	0.9	0.8	-

Table I Details of observations.

questions such as the nature of radiating particles, the connection between radio and  $\gamma$ -ray emission, the location of emitting regions and the origin of the flux variability. Very long baseline interferometry (VLBI) plays an important role in addressing these scientific questions because it is the only technique that can resolve (at least partially) the inner structure of the jet. Therefore, cross-correlation studies of VLBA data with data from other energy ranges (in particular  $\gamma$  rays) can provide us with important information about the structure of the jet and the location of the blazar emission.

## 2. Observations

We have new observations of Mrk 421 made throughout 2011 with the VLBA. The source was observed once per month, for a total of 12 epochs, at three frequencies: 15, 23.8 and 43 GHz. In each epoch Mrk 421 has been observed for nearly 40 minutes. We also observed, with regular intervals, three other sources (J0854+2006, J1310+3220 & J0927+3902) used as calibrators. In this paper we present a preliminary analysis of the first seven epochs of observations (from January to July) at 15 and 23.8 GHz. For calibration and fringe-fitting we used the AIPS software package [8], and for map production we used standard self-calibration procedures included in the DIFMAP software package [9]. In some epochs one or more antennas did not work properly, because of technical problems or bad weather conditions. For a complete report, see Table I.

## 3. Results

### 3.1. Images

Images at 15 and 23.8 GHz for the first seven epochs created with DIFMAP are shown in Figs.1 and 2. In all maps at these frequencies Mrk 421 shows a well defined and well collimated jet structure (one-sided

jet) emerging from a compact nuclear region (core-dominated source). This is the typical structure of a BL Lac object [10]. The jet extends for roughly 4.5 mas (2.67 pc), with a position angle slightly less than 45 deg in the northwest direction.

### 3.2. Model fits

For each epoch we used the model-fitting routine in DIFMAP to fit the brightness distribution of the source in the u-v plane with elliptical or circular Gaussian components. In this manner we can investigate in detail the inner jet structure and its evolution. In all epochs at 15 GHz a good fit is obtained with five Gaussian components. At 23.8 GHz we have identified six components: thanks to the increased angular resolution, the second innermost component (0.45 mas from the core, which we identify with the brightest, innermost and most compact component) is resolved into two features (at 0.3 mas and 0.7 mas from the core).

At 15 GHz we label components with C1, C2, C3, C4, starting from the outermost (C1) to the innermost (C4). At 23.8 GHz the C4 component is split into C4a and C4b. Overall, the components extend up to a region of about 5 mas. In this way, with a limited number of components, it is possible to analyze proper motions at various times and flux levels. From Fig.3 we can clearly see that data occupy well-defined areas in the plane, and this behavior supports the identification of individual components across epochs. However this choice is not unique, so it is useful to confirm with the analysis of flux variations discussed in the next section. We will investigate all these aspects in more detail in a further analysis of data at 43 GHz.

### 3.3. Flux density variations

Using the modelfit it is also possible to analyze the temporal evolution of the flux for each component of the source. The brightest component is the one describing the nuclear region (core-dominated source);

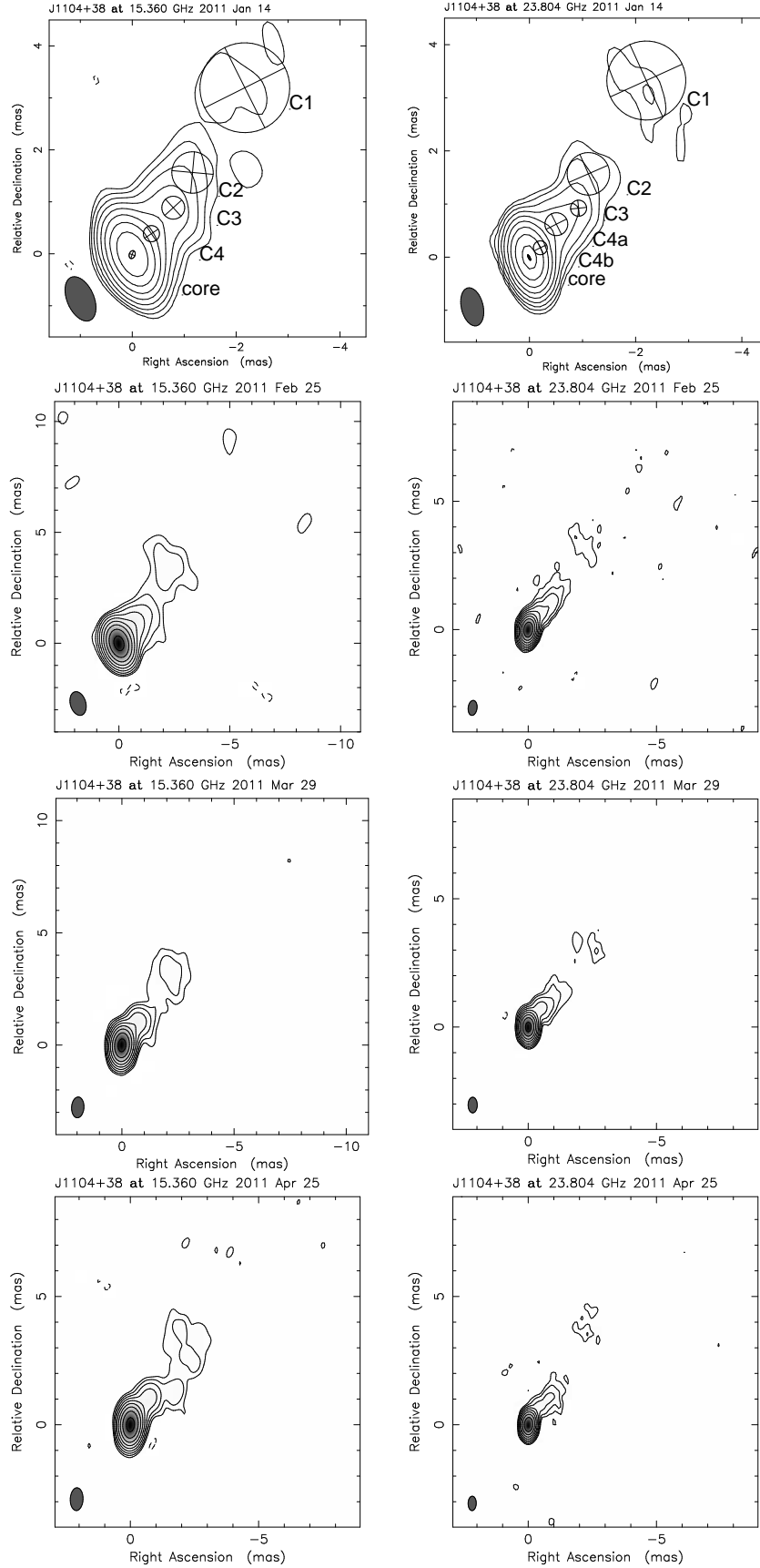


Figure 1: Images of Mrk 421 from January to April. The left and right panels show 15 and 23.8 GHz images respectively. The restoring beam and the lowest contours for each image are given in Table I. Levels are drawn at  $(-1, 1, 2, 4, \dots) \times$  the lowest contour given in Table I.

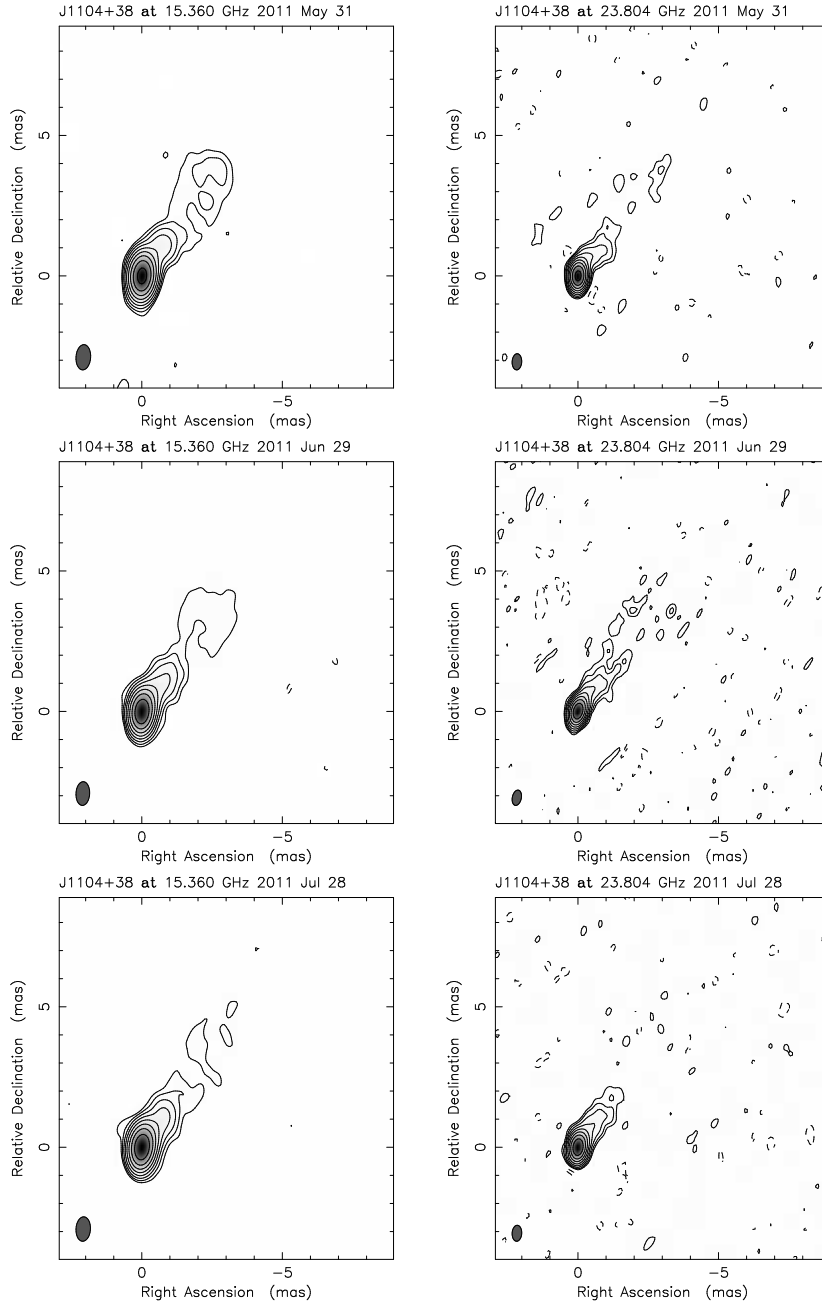


Figure 2: Images of Mrk 421 from May to July. The left and right panel show 15 and 23.8 GHz images respectively. The restoring beam and the lowest contours for each image are given in Table I. Levels are drawn at  $(-1, 1, 2, 4, \dots) \times$  the lowest contour given in Table I.

at 15 GHz it has a value around 350 mJy, which decreases along the jet as it moves away from the core, to values around 10 mJy. From a comparison of the flux density of each component at the various epochs it emerges that there is no significant variation in flux densities for both the core and for other components; the flux value for each component remains roughly constant at various times within the uncertainties calculated. Small variations may be artifacts brought about by our fitting procedures: e.g. the flux density

of inner components may be underestimated in some cases, because part of it was incorporated into the core component flux. This is a remarkable result because it allows the identification of components based on flux density values, and it confirms our choice of components based on their positions. A comparison to the lightcurves at higher frequencies, as well as the discussion of the spectral index structure, will be the subject of a future paper.

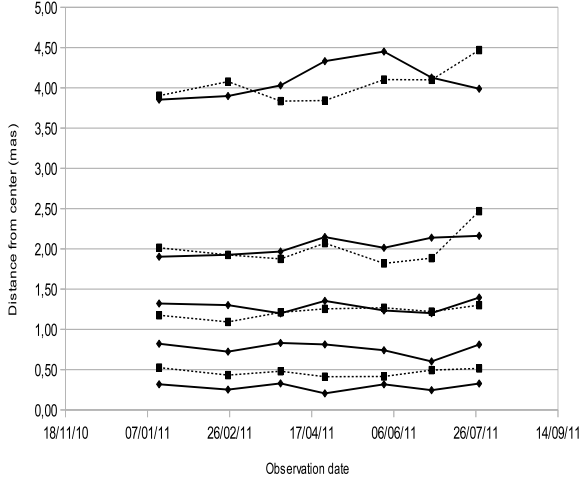


Figure 3: Results of model-fit analysis of the first seven epochs. Squares and diamonds refer respectively to positions of Gaussian components at 15 and 23.8 GHz. Solid (23.8 GHz) and dashed (15 GHz) lines between data are only for guidance. Error bars (not shown) are comparable with the positional scatter of each component. A proper treatment of the positional uncertainty, also accounting for core opacity effects, will be given in a forthcoming publication.

### 3.4. Apparent speeds

From our model fit we infer low or no displacement for the jet components. To quantify this value we have determined speeds for each component through linear fits to the separation of the individual features from the core in different epochs. For the three outer components (C1, C2 and C3), we used combined data at 15 and at 23.8 GHz, since the positions of each component at the two frequencies are consistent within the error bars; for the two inner components (C4a and C4b) we used only data at 23.8 GHz. Results are shown in Table II.

We find low values for the apparent speed, which agrees with previous studies [11]: the two innermost components (C4a and C4b) are consistent with being stationary; C2 and C3 have low-significance (1-2 $\sigma$ ) subluminal motion, and only the outermost component C1 shows superluminal motion, although only at 2.5 $\sigma$  confidence level. We will give a possible interpretation in the discussion section. It is important to emphasize that these are only partial results from a preliminary analysis; we can not exclude that they will change significantly in the conclusive analysis of the entire data set. We will give more accurate conclusions in a forthcoming paper.

Component	Apparent speed (mas/month)	$\beta_{app}$
C1	$0.06 \pm 0.02$	$1.3 \pm 0.5$
C2	$0.04 \pm 0.02$	$0.9 \pm 0.4$
C3	$0.01 \pm 0.01$	$0.3 \pm 0.2$
C4a	$-0.01 \pm 0.02$	$-0.3 \pm 0.4$
C4b	$0.00 \pm 0.01$	$0.0 \pm 0.2$

Table II Apparent speeds from linear fit analysis.

## 4. Discussion and conclusions

The trend of the measured velocities can be interpreted in different ways. If these apparent speeds, shown in Table II, represent the bulk apparent speed of the plasma in the jet, we can infer that some mechanism involving an acceleration acts in the outer region of the jet, resulting in a higher speed for the outermost component, e.g. C1. Alternatively we can invoke the presence of a transverse velocity structure along the jet axis. This structure consists of two components: a fast inner *spine* and a slower outer *layer*. Speeds are obtained depending on whether we are measuring the speed of the spine or the layer. In this way speeds reported in Table II are only pattern speeds, and we suggest that various blobs of plasma (components) that represent the jet's structure found by us do not represent moving structures. Therefore, measured velocities would not be intrinsically linked to the jet's bulk velocity.

Other variations of this model have been proposed [12, 13], and we expect to constrain the variability and the details of these models with the complete analysis of the whole dataset, giving our own interpretation. In any case, it is difficult to reconcile slow apparent speeds in the inner region of the jet with the high value for Doppler factor ( $\delta$ )<sup>1</sup> required from TeV variability. With the  $\delta$  dependence on both  $\beta$  and  $\theta$ , only very small viewing angles ( $\theta \sim 1^\circ$ ) are compatible with the measured apparent speeds. While it is true that such a value is not particularly surprising for a blazar, we note that similar (or even smaller) values for  $\beta_{app}$  are found for all the  $\sim 10$  TeV blazars that have proper motions reported in the literature [14, 15]. When angles of a small fraction of a degree are required for many sources, then the statistics are untenable, and the “Doppler crisis” for the TeV blazars can not be explained solely on the basis of small angles to the line of sight (see also [16]).

These findings might also be ascribed to the lack of high contrast features in the model fit. Most likely, the

<sup>1</sup> $\delta = 1/\gamma(1 - \beta \cos \theta)$ , where  $\gamma$  is the bulk Lorentz factor,  $\theta$  is the angle of view and  $\beta = v/c$ .

low apparent speed found implies that proper motion in this case does not give any information on the jet bulk velocity that, according to other evidence (jet sidedness, core dominance, and high energy emission), requires a relativistic jet velocity. Indeed, we plan to further constrain the jet velocity by means of a study of the jet sidedness ratio. We will present the entire analysis of constraints for these physical parameters in a forthcoming paper.

In summary, the preliminary analysis presented here has confirmed with high clarity the predictions made on the basis of knowledge so far achieved for TeV blazars. However, there is still much to be understood and we expect to obtain more significant results from the analysis of the entire dataset, particularly from 43 GHz data. Finally we could combine our data with those of other works [11] by increasing the temporal coverage of observations to obtain meaningful results over a longer time frame.

## Acknowledgments

This work is based on observations obtained through the BG207 VLBA project. The National Radio Astronomy Observatory is a facility of the National Science Foundation operated under cooperative agreement by Associated Universities, Inc.

## References

- [1] Punch, M., Akerlof, C. W., Cawley, M. F., et al. 1992, *Nature*, 358, 477
- [2] Abdo, A. A., Ackermann, M., Ajello, M., et al. 2011, *ApJ*, 736, 131
- [3] Tavecchio, F., Maraschi, L., Pian, E., et al. 2001, *ApJ*, 554, 725
- [4] Gaidos, J. A., Akerlof, C. W., Biller, S., et al. 1996, *Nature*, 383, 319
- [5] Giroletti, M., Giovannini, G., Taylor, G. B., & Falomo, R. 2006, *ApJ*, 646, 801
- [6] Piner, B. G., Unwin, S. C., Wehrle, A. E., et al. 1999, *ApJ*, 525, 176
- [7] Piner, B. G., & Edwards, P. G. 2004, *ApJ*, 600, 115
- [8] Greisen, E. W. 2003, *Astrophys. Space Sci. Libr.*, 285, 109
- [9] Shepherd, M. C. 1997, in *ASP Conf. Ser. 125, Astronomical Data Analysis Software and Systems VI*, ed. G. Hunt & H. E. Payne (San Francisco, CA: ASP), 77
- [10] Giroletti, M., Giovannini, G., Taylor, G. B., & Falomo, R. 2004, *ApJ*, 613, 752
- [11] Piner, B. G., & Edwards, P. G. 2005, *ApJ*, 622, 168
- [12] Giroletti, M., Giovannini, G., Feretti, L., et al. 2004, *ApJ*, 600, 127
- [13] Ghisellini, G., Tavecchio, F., & Chiaberge, M. 2005, *AAP*, 432, 401
- [14] Piner, B. G., Pant, N., & Edwards, P. G. 2008, *ApJ*, 678, 64
- [15] Piner, B. G., Pant, N., & Edwards, P. G. 2010, *ApJ*, 723, 1150
- [16] Lyutikov, M., & Lister, M. 2010, *ApJ*, 722, 197